

MoE-Spec: Expert Budgeting for Efficient Speculative Decoding

Bradley McDanel^{1,2} Steven Li² Sruthikesh Surineni² Harshit Khaitan²

Abstract

Speculative decoding accelerates Large Language Model (LLM) inference by verifying multiple drafted tokens in parallel. However, for Mixture-of-Experts (MoE) models, this parallelism introduces a severe bottleneck: large draft trees activate many unique experts, significantly increasing memory pressure and diminishing speedups from speculative decoding relative to autoregressive decoding. Prior methods reduce speculation depth when MoE verification becomes expensive. We propose MoE-Spec, a training-free verification-time expert budgeting method that decouples speculation depth from memory cost by enforcing a fixed expert capacity limit at each layer, loading only the experts that contribute most to verification and dropping the long tail of rarely used experts that drive bandwidth overhead. Experiments across multiple model scales and datasets show that this method yields 10–30% higher throughput than state-of-the-art speculative decoding baselines (EAGLE-3) at comparable quality, with flexibility to trade accuracy for further latency reductions through tighter budgets.

1. Introduction

Mixture-of-Experts (MoE) models have become the dominant architecture for state-of-the-art language models, powering systems such as GPT-4 (Achiam et al., 2023), DeepSeek-R1 (Guo et al., 2025), and Llama-4 (Meta AI, 2025). MoEs reduce inference cost through sparse activation: each token activates only k of the N total experts per layer, so memory bandwidth scales with active rather than total parameters. Speculative decoding accelerates LLM inference by verifying multiple drafted tokens in parallel (Leviathan et al., 2023; Chen et al., 2023). For dense models, this parallelism is essentially free: all parameters are loaded once per forward pass, so verification cost is constant regardless of draft size.

¹Franklin and Marshall College ²Meta Reality Labs. Correspondence to: Bradley McDanel <bmcdanel@fandm.edu>.

Preprint. February 19, 2026.

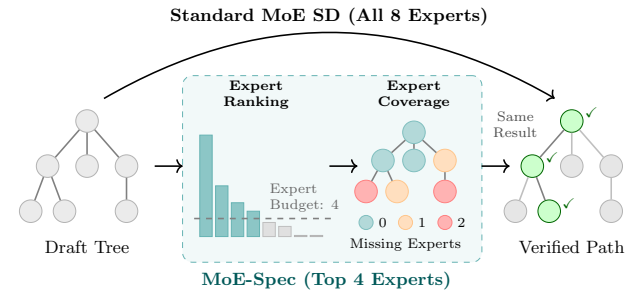


Figure 1. Overview of MoE-Spec. Standard MoE speculative decoding loads all N experts ($N = 8$) activated across the draft tree (top path). MoE-Spec ranks experts by aggregate routing probability and enforces a budget B (here $B = 4$), loading only top-scoring experts (bottom path). Tokens are color-coded by the number of missing experts from their natural routing. In this example, both paths accept the same three tokens despite MoE-Spec loading half as many experts.

For MoE models, verification cost is no longer constant: it scales with the diversity of expert activations across the draft tree. Each token routes independently to its own subset of experts, and the target model must load the *union* of all selected experts to verify the tree (Figure 2a). As draft size grows, so does the number of unique experts: on OLMoE-1B-7B, a 127-token tree activates 54 of 64 experts per layer, approaching the full model (Figure 2b). Verification can thus become more expensive than autoregressive decoding, negating both the benefits of sparse activation and speculation.

However, not all experts in the union contribute equally to verification. Expert activations across a draft tree follow a heavy-tailed distribution (Figure 2c): on OLMoE, the top 32 of 64 experts capture 93% of aggregate routing probability. The remaining experts incur bandwidth cost but contribute little to output quality. This asymmetry suggests that verification cost can be reduced without proportional quality loss by enforcing an expert budget: loading only the highest-scoring experts and dropping the long tail.

We propose MoE-Spec, a method that enforces a strict expert budget during verification (Figure 1). Given a draft tree, we aggregate routing probabilities across all tokens and select the top- B experts to form a shortlist. Tokens whose natural routing falls outside the shortlist are handled by truncation (omitting missing experts) or substitution (re-

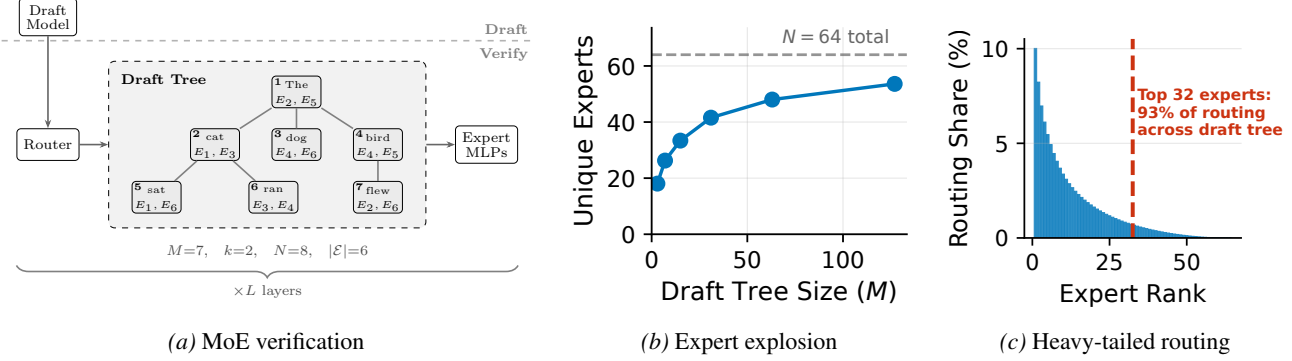


Figure 2. Motivation for expert budgeting. (a) During verification, each token routes to k experts; the target model must load all unique experts \mathcal{E} across the draft tree. (b) As tree size M grows, unique experts per layer approaches N , negating sparse activation benefits. (c) Routing probabilities are heavy-tailed: the top 32 of 64 experts capture 93% of routing weight for a tree size of 63.

placing them with available alternatives). This decouples verification cost from draft tree complexity: regardless of tree size, we load at most B experts per layer. We explore three ranking strategies: static (fixed ordering from calibration), router-based (aggregating routing probabilities per tree), and an Oracle upper bound that greedily minimizes reconstruction error.

We evaluate MoE-Spec on three MoE architectures (OLMoE-1B-7B, Qwen3-30B-A3B, Mixtral-8x7B) across mathematical reasoning, code generation, and summarization tasks. Compared to EAGLE-3 (Li et al., 2025), MoE-Spec achieves 10–30% higher throughput at comparable quality, with flexibility to trade accuracy for further speedup through tighter budgets. Our main contributions are:

- We show that expert activations during MoE verification are heavy-tailed, with a small subset capturing most routing weight across the draft tree.
- We propose MoE-Spec, a simple yet effective method that enforces an expert budget during verification by selecting a budgeted subset of these top-scoring experts. Unlike prior work that requires architectural changes or additional training, our approach is training-free and integrates directly into existing speculative decoding pipelines.
- We demonstrate throughput improvements over EAGLE-3 across three MoE architectures spanning different scales and expert configurations.
- Our Oracle analysis indicates that improved ranking could reduce expert requirements by 25% over our router-based heuristic, motivating future work on better selection methods.

2. Background

2.1. Mixture-of-Experts

Mixture-of-Experts (MoE) models achieve parameter efficiency by activating only a subset of model weights for each token. In an MoE layer, the standard feed-forward network is replaced with N parallel expert networks $\{E_1, \dots, E_N\}$ and a learned router that selects k experts to process each token (where $k \ll N$).

Given a token representation $\mathbf{h} \in \mathbb{R}^d$, the router computes a probability distribution over experts via a linear projection followed by softmax.¹

$$g_i(\mathbf{h}) = \frac{\exp(\mathbf{w}_i^\top \mathbf{h})}{\sum_{j=1}^N \exp(\mathbf{w}_j^\top \mathbf{h})}, \quad (1)$$

where $\mathbf{w}_i \in \mathbb{R}^d$ is the routing weight vector for expert i . Let $\mathcal{T}_k(\mathbf{h}) \subset \{1, \dots, N\}$ denote the indices of the top- k experts by routing probability. The MoE layer output is a weighted combination of the selected experts:

$$\text{MoE}(\mathbf{h}) = \sum_{i \in \mathcal{T}_k(\mathbf{h})} \bar{g}_i(\mathbf{h}) \cdot E_i(\mathbf{h}), \quad (2)$$

where $\bar{g}_i(\mathbf{h})$ denotes the mixing weights. These are either the raw routing probabilities $g_i(\mathbf{h})$ or renormalized values $g_i(\mathbf{h}) / \sum_{j \in \mathcal{T}_k(\mathbf{h})} g_j(\mathbf{h})$, depending on the architecture (e.g., OLMoE renormalizes; Qwen3 does not).

This sparse activation pattern means that inference cost scales with the number of *active* parameters rather than total parameters. For a single token, only k experts (typically $k \in \{2, 8\}$) are loaded from memory. However, when processing multiple tokens jointly, the model must load the *union* of experts selected across all tokens, which can approach the full set of N experts as token count grows.

¹Some architectures, such as DeepSeek-V3, use sigmoid-based routing instead. Our method applies to both, though we focus on softmax-routed models in experiments.

2.2. Speculative Decoding with Draft Trees

Speculative decoding accelerates autoregressive generation by drafting multiple candidate tokens and verifying them in parallel (Leviathan et al., 2023; Chen et al., 2023). A lightweight *draft model* proposes candidate continuations, and the full *target model* verifies these candidates in a single forward pass. Accepted tokens are emitted immediately; rejected tokens trigger resampling from a corrected distribution. This process is provably lossless for greedy decoding as the output distribution matches standard autoregressive decoding.

Modern methods such as EAGLE (Li et al., 2024b;c) extend this to *tree-structured* drafts, where multiple candidate tokens are proposed at each position. The target model verifies all candidates simultaneously using tree attention, accepting a path of tokens consistent with the target distribution.

For dense models, verification cost is effectively constant regardless of draft tree size: all model parameters are loaded once per forward pass, and the additional compute for extra tokens is negligible in the memory-bound regime. This makes aggressive speculation attractive—larger trees increase the expected number of accepted tokens per iteration. For MoE models, however, this assumption breaks down; we analyze this problem in Section 3.1.

3. Method

3.1. Verification Overhead in Tree Decoding

As described in Section 1, MoE verification cost scales with expert diversity across the draft tree. We formalize this as follows. Let $\mathcal{D} = \{\mathbf{h}_1, \dots, \mathbf{h}_M\}$ denote a draft tree of M token representations. To verify the tree, the target model must load the union of all selected experts:

$$\mathcal{E}(\mathcal{D}) = \bigcup_{t=1}^M \mathcal{T}_k(\mathbf{h}_t). \quad (3)$$

As Figure 2b shows, $|\mathcal{E}|$ approaches N for large trees, negating sparse activation benefits. However, expert routing is heavy-tailed (Figure 2c): by enforcing a budget $B < |\mathcal{E}|$ and loading only the highest-scoring experts, we reduce bandwidth while preserving verification quality.

3.2. Expert Importance Ranking

Given an expert budget $B < N$, we select a shortlist \mathcal{S} of B experts to load during verification. We consider three ranking strategies.

Static Ranking. The simplest approach precomputes a fixed ordering from calibration data by counting selection

frequency:

$$c_i = \sum_{\mathbf{h} \in \text{calib}} \mathbf{1}[i \in \mathcal{T}_k(\mathbf{h})]. \quad (4)$$

The shortlist consists of the B experts with highest c_i . This incurs zero runtime overhead and enables permanent model pruning—deploying only 32 of 64 experts halves memory requirements. At moderate budgets ($B \geq N/2$), static ranking performs comparably to adaptive methods on most tasks (Section 4.6). The gap widens at aggressive budgets, where input-dependent routing becomes more valuable.

Router-Based Ranking. Our primary method aggregates routing probabilities across the draft tree:

$$s_i = \sum_{t=1}^M g_i(\mathbf{h}_t). \quad (5)$$

The shortlist \mathcal{S} consists of the B experts with highest s_i . This requires no computation beyond what the router already produces, and adapts to each tree’s routing pattern.

Oracle Ranking. As an upper bound, we consider an oracle with access to the target model’s routing decisions and expert outputs. The oracle greedily selects experts to minimize reconstruction error against the unpruned output. Let $O^* = \sum_{i \in \mathcal{T}_k(\mathbf{h}_t)} g_i(\mathbf{h}_t) \cdot E_i(\mathbf{h}_t)$ denote the gold output. Starting from $\mathcal{S} = \emptyset$, the oracle iteratively adds the expert i^* that minimizes:

$$i^* = \arg \min_{i \notin \mathcal{S}} \sum_{t=1}^M \left\| O_t^* - \sum_{j \in \mathcal{S} \cup \{i\}} g_j(\mathbf{h}_t) \cdot E_j(\mathbf{h}_t) \right\|_2^2. \quad (6)$$

This requires running all experts and is impractical for speedup, but provides a ceiling on achievable quality.

3.3. Expert Coverage

Given shortlist \mathcal{S} , we must handle tokens whose natural routing includes experts outside \mathcal{S} . We consider two policies.

Truncation. Each token uses its natural top- k routing, but experts outside \mathcal{S} contribute zero:

$$\text{MoE}_{\mathcal{S}}^{\text{trunc}}(\mathbf{h}_t) = \sum_{i \in \mathcal{T}_k(\mathbf{h}_t) \cap \mathcal{S}} \bar{g}_i(\mathbf{h}_t) \cdot E_i(\mathbf{h}_t). \quad (7)$$

Probabilities \bar{g}_i are computed over the original top- k set (not re-computed for the reduced set). Tokens whose natural routing overlaps partially with \mathcal{S} receive fewer than k experts. In the extreme case where $\mathcal{T}_k(\mathbf{h}_t) \cap \mathcal{S} = \emptyset$, the MoE output is zero and only the residual connection passes through. This effectively skips the MoE computation for that token at that layer.

Substitution. Top- k selection is constrained to \mathcal{S} . Let $\mathcal{T}_k^{\mathcal{S}}(\mathbf{h}_t)$ denote the top- k experts within \mathcal{S} , ranked by $g_i(\mathbf{h}_t)$:

$$\text{MoE}_{\mathcal{S}}^{\text{sub}}(\mathbf{h}_t) = \sum_{i \in \mathcal{T}_k^{\mathcal{S}}(\mathbf{h}_t)} \bar{g}_i^{\mathcal{S}}(\mathbf{h}_t) \cdot E_i(\mathbf{h}_t), \quad (8)$$

where $\bar{g}_i^{\mathcal{S}}$ are the routing probabilities over the constrained selection. If a token’s natural top- k includes experts outside \mathcal{S} , those experts are replaced by the highest-scoring available alternatives within the shortlist. Every token receives exactly k experts, though they may differ from natural routing. We compare both policies empirically in Section 4.4.

4. Experiments

4.1. Experimental Setup

Models. We evaluate on three MoE architectures spanning different scales and expert configurations: OLMoE-1B-7B (Muennighoff et al., 2024), with 64 experts and $k = 8$ active per token (7B total, 1B active parameters); Qwen3-30B-A3B, with 128 experts and $k = 8$ (30B total, 3B active); and Mixtral-8x7B (Jiang et al., 2024), with 8 experts and $k = 2$ (47B total, 13B active). For speculative decoding, we use EAGLE-3 (Li et al., 2025) draft models for OLMoE and Qwen3, and the original EAGLE (Li et al., 2024b) for Mixtral.

Benchmarks. We evaluate on five benchmarks spanning mathematical reasoning, code generation, and summarization. GSM8K and MATH500 test multi-step arithmetic and competition-level math problems respectively, measured by accuracy. HumanEval and MBPP evaluate code generation via pass@1 on function synthesis tasks. CNN/DailyMail tests abstractive summarization, measured by ROUGE-L F1.

Baselines. We compare against two baselines: autoregressive decoding (AR), which generates tokens sequentially without speculation, and EAGLE, the current state-of-the-art for tree-structured speculative decoding. We use EAGLE-3 for OLMoE and Qwen3, and EAGLE-1 for Mixtral where EAGLE-3 draft models are unavailable. All draft model adapters are from the official EAGLE repository.

Implementation. We implement MoE-Spec by extending the EAGLE-3 codebase² to add expert budgeting during the verification phase (Section B). We use the open-source EAGLE-3 implementation without modification to tree construction or verification; our only change is batched MoE computation for efficiency (Section C). All main results use router-based expert selection with the substitution policy; ablations over selection methods and coverage policies

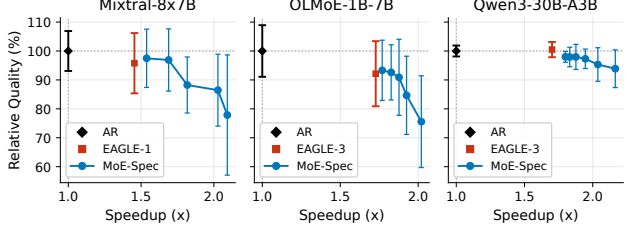


Figure 3. Quality-speedup tradeoff at $T = 1$, averaged across five benchmarks. For each benchmark, quality and speedup are normalized relative to AR (100%), then averaged. Error bars combine cross-benchmark variance with seed-to-seed variance from 5 runs. Individual per-benchmark curves appear in Section E.

appear in Section 4.4. Following Li et al. (2025), we use draft trees of 63 tokens and evaluate at both temperature 0 (greedy decoding) and temperature 1 (sampling).³ Full hyperparameters and model configurations are in Section A.

4.2. Main Results

MoE-Spec improves speedup over EAGLE in 27 of 30 model-benchmark configurations while maintaining comparable quality. Table 1 compares autoregressive decoding (AR), EAGLE, and MoE-Spec across three MoE architectures and five benchmarks at both $T = 0$ and $T = 1$. For MoE-Spec, we select the expert budget that maximizes throughput while keeping quality within one standard deviation of EAGLE (measured from $T = 1$ runs with 5 seeds). As a concrete example, on Mixtral MBPP at $T = 0$, MoE-Spec achieves $2.3 \times$ speedup compared to EAGLE’s $1.7 \times$, a 35% relative improvement at identical task accuracy.

Larger models show greater relative improvements from expert budgeting. Mixtral-8x7B (14B active parameters) averages 27% relative speedup gain over EAGLE across both temperatures. Qwen3-30B-A3B (3B active) averages 16%, and OLMoE-1B-7B (1B active) averages 6%. MoE-Spec achieves similar acceptance lengths to EAGLE despite loading fewer experts, with only a 1.4% reduction on average across all configurations. Since acceptance rates remain nearly unchanged, the speedup gains come entirely from reduced verification cost per step.

Given this robustness, the expert budget becomes a practical control surface for balancing quality against latency. Figure 3 shows the tradeoff at $T = 1$: for each benchmark, we normalize quality and speedup relative to AR, then average across all five benchmarks. Unlike EAGLE, which provides a single operating point, MoE-Spec traces a continuous

³Lossless speculative decoding requires rejection sampling with draft probability $q(x)$ (Leviathan et al., 2023). For tree-based methods, computing $q(x)$ requires tracking probabilities across all paths. The EAGLE implementation uses $q(x) = 1$, which causes the distribution shift we observe at $T=1$. MoE-Spec inherits this, so comparisons remain valid.

²<https://github.com/SafeAILab/EAGLE>

Table 1. Speedup over autoregressive decoding, mean acceptance length (τ), and task metrics at T=0 and T=1. MoE-Spec uses substitution policy with the expert budget maximizing throughput while maintaining quality comparable to EAGLE-3 (within one standard deviation, measured from T=1 runs with 5 seeds). T=1 results report mean over 5 random seeds.

Model	Method	GSM8K			MATH500			HumanEval			MBPP			CNN/DM		
		Spd	Acc	τ	Spd	Acc	τ	Spd	P@1	τ	Spd	P@1	τ	Spd	R-L	τ
Temperature = 0																
Mixtral-8x7B	AR	1.0×	39	—	1.0×	31	—	1.0×	22	—	1.0×	56	—	1.0×	18	—
	EAGLE	1.5×	46	2.8	1.4×	31	2.5	1.6×	20	3.2	1.7×	45	3.2	1.3×	18	2.3
	MoE-Spec	1.8×	44	2.9	2.0×	34	2.5	1.9×	27	3.1	2.3×	45	3.1	1.5×	18	2.2
OLMoE-1B-7B	AR	1.0×	74	—	1.0×	28	—	1.0×	30	—	1.0×	45	—	1.0×	18	—
	EAGLE-3	1.6×	69	3.0	2.1×	26	3.6	2.3×	30	4.2	2.2×	45	4.0	1.2×	17	2.0
	MoE-Spec	1.7×	66	3.0	2.5×	28	3.5	2.4×	30	4.2	2.2×	46	3.8	1.3×	18	2.0
Qwen3-30B-A3B	AR	1.0×	86	—	1.0×	82	—	1.0×	82	—	1.0×	90	—	1.0×	16	—
	EAGLE-3	1.9×	85	3.2	1.8×	81	3.0	1.8×	82	3.1	1.7×	89	2.9	1.5×	17	2.1
	MoE-Spec	2.4×	84	3.2	2.2×	81	2.9	2.2×	78	3.1	1.7×	89	2.9	1.9×	16	2.0
Temperature = 1																
Mixtral-8x7B	AR	1.0×	44	—	1.0×	30	—	1.0×	21	—	1.0×	57	—	1.0×	18	—
	EAGLE	1.5×	42	2.8	1.4×	30	2.5	1.6×	21	3.1	1.6×	48	3.1	1.2×	18	2.2
	MoE-Spec	2.1×	40	2.8	1.6×	31	2.5	1.9×	20	3.1	1.8×	50	3.1	1.8×	18	2.1
OLMoE-1B-7B	AR	1.0×	60	—	1.0×	26	—	1.0×	29	—	1.0×	41	—	1.0×	15	—
	EAGLE-3	1.7×	49	3.2	1.9×	22	3.4	2.0×	26	3.6	2.0×	40	3.5	1.0×	16	1.4
	MoE-Spec	1.9×	53	3.1	2.1×	26	3.2	2.0×	29	3.8	2.0×	42	3.5	1.0×	15	1.4
Qwen3-30B-A3B	AR	1.0×	84	—	1.0×	79	—	1.0×	81	—	1.0×	88	—	1.0×	16	—
	EAGLE-3	1.8×	87	3.2	1.8×	79	2.9	1.8×	80	3.0	1.7×	89	2.9	1.5×	16	2.0
	MoE-Spec	2.1×	84	3.2	2.3×	79	2.8	1.9×	78	3.0	1.7×	89	2.9	1.7×	16	2.0

Pareto curve from conservative (high budget, near-EAGLE quality) to aggressive (low budget, higher speedup). This enables applications to select operating points tailored to their quality requirements.

The quality degradation profile varies across models. Qwen3-30B-A3B shows the most favorable tradeoff, maintaining approximately 95% quality even at $2.0\times$ speedup with tight error bars. Mixtral-8x7B exhibits moderate degradation, with quality dropping to approximately 78% at maximum speedup. OLMoE-1B-7B shows the steepest decline and highest variance at aggressive speedup targets, consistent with smaller models being more sensitive to approximations. Table 1 reports one point on each curve: the budget that maximizes speedup while staying within quality tolerance. Individual per-benchmark curves appear in Section E.

4.3. Speedup Analysis

The speedup gains in Table 1 arise because MoE-Spec loads at most B experts per layer while EAGLE-3 must load all experts activated across the draft tree, even those used by only a minority of tokens (Figure 2c). Figure 4 illustrates this effect on OLMoE-1B-7B at a fixed expert budget $B = 32$ as a function of tree size. For this experiment, we aggregate across all 5 datasets outlined in Section 4.1. Figure 4a shows that the average active number of experts per draft tree is

significantly smaller for MoE-Spec compared to EAGLE-3 even at moderate tree sizes. For example, at tree size of 31, MoE-Spec uses on average 29 experts compared to 39 for EAGLE-3. At larger tree sizes, this gap widens: MoE-Spec saturates at 32 experts while EAGLE-3 approaches using all 64 experts per tree.

The speedup for EAGLE peaks at tree size 31 then declines as straggler experts dominate verification cost, while MoE-Spec continues improving throughout (Figure 4b). Both methods achieve similar gains at small tree sizes where expert counts remain low. Beyond tree size 15, EAGLE peaks at $1.95\times$ then declines to $1.85\times$ at tree size 255. The memory bandwidth cost of loading straggler experts, those activated by only a few tokens in the tree, outpaces the benefit from longer accepted sequences. MoE-Spec avoids this overhead and continues improving throughout, reaching $2.1\times$ at tree size 255.

The relationship between speedup and active experts reveals a saturation point around 32 experts, beyond which additional loading yields diminishing returns. Figure 4c shows this by plotting speedup against active experts directly. EAGLE operates past this saturation point at large tree sizes, reaching 54 experts at tree size 255, while MoE-Spec stays below it by construction. The experts beyond the saturation point are stragglers from the tail of the routing distribution: they serve only a handful of tokens in each draft tree but

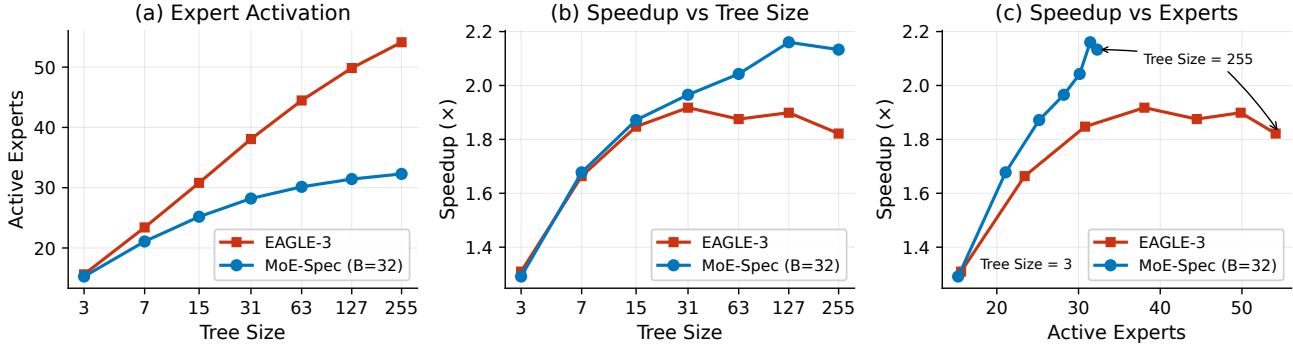


Figure 4. Expert activation and speedup on OLMoE-1B-7B. (a) Unique experts activated during verification as tree size increases. EAGLE-3 loads over 50 of 64 experts at large trees; MoE-Spec with $B = 32$ saturates at the budget. (b) Speedup relative to AR. EAGLE-3 peaks at tree size 31 then declines as expert loading dominates; MoE-Spec continues improving at larger trees. (c) Speedup vs. active experts. At tree size 255, EAGLE-3 loads 54 experts for $1.85\times$ speedup; MoE-Spec loads 32 experts for $2.1\times$ speedup.

incur the same memory bandwidth cost as the heavily-used experts. Expert budgeting excludes them from verification, keeping cost bounded while preserving the high-value experts that dominate routing probability (Figure 2c). The selection overhead (computing routing probabilities and sorting to form the shortlist) consumes only 2–3% of total generation time, far smaller than the verification savings from reduced expert loading.

The robustness to aggressive budgets follows from the routing distribution: at $B = 32$, the excluded experts collectively receive only 7% of routing weight across the draft tree. The router’s own probability assignments identify which experts matter, and budgeting simply enforces that judgment. For tokens whose preferred experts fall outside the shortlist, substitution provides alternative experts while truncation relies on the residual connection to preserve the hidden state.

4.4. Ablation Studies

We evaluate the impact of the expert selection strategy on generation quality across varying budgets. Figure 5a compares three ranking methods using the Substitution coverage policy: Router-based (aggregating routing probabilities across the draft tree), Static (fixed ordering from calibration data), and Oracle (greedy selection using target model outputs). Static ranking fails at low budgets ($B \leq 16$), achieving near-zero accuracy on GSM8K and MATH500 because a fixed expert set cannot adapt to input variability. Router-based ranking remains robust across the budget range, tracking the Oracle upper bound even at tight budgets.

The Oracle method achieves near-AR quality even at $B = 24$ (37.5% of experts), suggesting room for improved selection strategies. While the Oracle is impractical for acceleration (it requires executing the full model to obtain routing decisions), better selection methods could close the remaining gap between Router and Oracle. Router-based

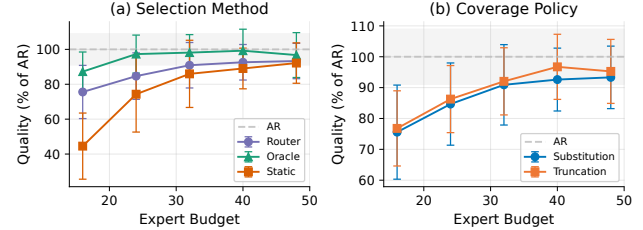


Figure 5. Design ablations on OLMoE-1B-7B at $T = 1$, normalized to autoregressive (AR) baseline. (a) Selection methods: Static ranking fails at low budgets while Router-based ranking tracks the Oracle upper bound. (b) Coverage policies: Truncation and Substitution perform comparably across budgets.

ranking offers the best practical tradeoff: it incurs no additional model execution cost while outperforming Static ranking by a wide margin at low budgets, and converging to within 5–10% of AR at moderate budgets ($B \geq 32$). We use Router-based ranking as the default.

Figure 5b examines how to handle tokens whose preferred experts fall outside the selected budget, using Router-based selection. Truncation zeros out missing experts while preserving natural routing weights; Substitution replaces missing experts with the highest-scoring available alternatives within the shortlist. Both policies perform comparably across all benchmarks and expert budgets. We select Substitution as the default to maintain a constant number of active experts (k) per token.

4.5. Reconstruction Error Analysis

Router-based ranking tracks but does not match Oracle across the budget range. To understand this gap, we measure reconstruction error: the normalized squared distance between the budgeted MoE output O_S and the full output O^* from Equation (2). We compute this at each MoE layer during Oracle selection, where all expert outputs are available,

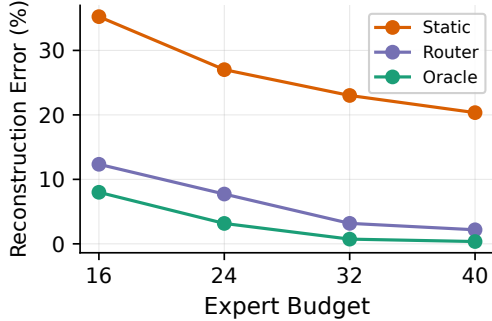


Figure 6. Reconstruction error by selection method on OLMoE-1B-7B, averaged across all MoE layers and 5 benchmarks. Oracle matches Router error using 25% fewer experts.

and average across layers and datasets.

Oracle achieves the same reconstruction error as Router while using 25% fewer experts (Figure 6). At $B = 24$, Oracle matches Router at $B = 32$ (both 3.2% error); at $B = 16$, Oracle nearly matches Router at $B = 24$ (8.0% vs. 7.7%). Static selection incurs 20–35% error regardless of budget. This 25% reduction in required experts explains why Oracle maintains quality at lower budgets in Figure 5a.

The gap stems from how each method allocates budget. Router-based selection scores each expert independently by summing routing probabilities across the draft tree. This ignores interactions: if two experts frequently co-activate (e.g., appear together across a draft tree), their contributions to the output are correlated, and selecting both yields diminishing marginal returns. Oracle selection, by contrast, picks experts greedily to minimize reconstruction error. After selecting an expert, the next addition is whichever expert most reduces the residual error. Experts correlated with those already selected provide less marginal benefit and are passed over.

Our profiling shows that routing is concentrated: certain expert pairs co-activate 10–30× more often than uniform-random selection would predict (averaging 23× across layers; see Section D for details). This concentration is why Oracle matches Router quality with 25% fewer experts. Router spends budget on popular experts with correlated contributions; Oracle does not. This suggests that selection methods modeling expert co-activation patterns, rather than treating experts independently, could close the gap without requiring full model execution.

4.6. Expert Coverage Across Datasets

We profile expert routing on each dataset by running the target model on calibration samples and recording routing probabilities for draft trees of size 63. Figure 7 shows cumulative routing probability captured by the top- B experts.

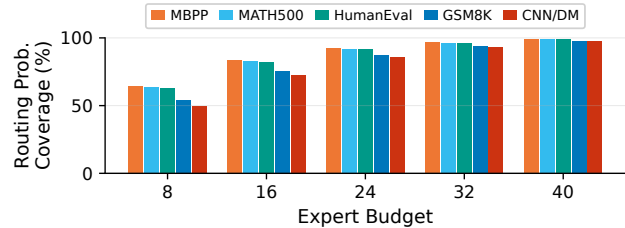


Figure 7. Routing probability coverage by expert budget across datasets on OLMoE-1B-7B with tree size 63. Datasets are ordered by coverage (best to worst): MBPP reaches 95% coverage with 8 experts, while CNN/DM requires 24 experts to reach 90%.

Routing concentration varies across tasks. Code generation (MBPP, HumanEval) concentrates on few experts: the top 8 capture over 90% of routing probability. Summarization (CNN/DM) spreads routing more broadly, requiring 24 experts to reach 90%.

Static ranking uses a fixed expert ordering from calibration data. When routing is concentrated, the same experts dominate across inputs, so a fixed ordering works well. When routing is dispersed, different inputs select different experts, and a fixed ordering misses task-specific patterns. Router-based selection sidesteps this by aggregating probabilities per draft tree.

5. Related Work

Speculative Decoding. Speculative decoding accelerates autoregressive generation by drafting candidate tokens with a lightweight model and verifying them in parallel with the target model (Leviathan et al., 2023; Chen et al., 2023). Subsequent work improved draft quality through learned drafters: EAGLE (Li et al., 2024b) predicts future hidden states autoregressively, EAGLE-2 (Li et al., 2024c) introduces dynamic draft trees based on confidence, and EAGLE-3 (Li et al., 2025) scales performance through training-time test. Medusa (Cai et al., 2024) adds multiple decoding heads for parallel token prediction. These methods assume verification cost is constant, which holds for dense models but breaks down for MoEs.

Mixture-of-Experts. The sparse MoE architecture routes each token to a subset of expert networks, reducing compute while maintaining model capacity (Shazeer et al., 2017). Switch Transformers (Fedus et al., 2022) established the modern paradigm of top- k routing in Transformers, which subsequent architectures including Mixtral (Jiang et al., 2024) and OLMoE (Muennighoff et al., 2024) adopted. On the systems side, MegaBlocks (Gale et al., 2023) provides efficient GPU kernels for MoE computation by avoiding padding through block-sparse operations. Our work targets a different bottleneck: the memory bandwidth cost of

loading experts during speculative verification.

Dynamic Sparsity. Dense LLMs exhibit heavy-tailed activation patterns: a small fraction of neurons accounts for most of the computation’s effect on output quality. Deja Vu (Liu et al., 2023) exploits this by training a predictor to identify contextual sparsity at runtime, skipping MLP and attention head computations unlikely to affect the output. PowerInfer (Song et al., 2024) partitions neurons into “hot” (frequently activated) and “cold” sets based on their Zipfian activation distribution, enabling efficient CPU-GPU hybrid inference by keeping hot neurons on GPU. Both methods target single-token inference in dense models, predicting which neurons to skip for each token independently.

MoE-Spec applies the same principle to a different setting: batched verification in sparse models. Rather than predicting sparsity per token, we aggregate routing probabilities across the draft tree and select experts that collectively cover the batch. This aggregation is key: individual tokens may route to diverse experts, but the distribution over the full tree is heavy-tailed (Figure 2c). Unlike Deja Vu and PowerInfer, we require no learned predictor; the router provides importance scores directly.

MoE Compression. MoE-Spec’s expert budgeting operates at inference time and is orthogonal to methods that reduce model size permanently. MoE-Pruner (Xie et al., 2024) prunes weights within experts, while other approaches merge experts (Li et al., 2024a) or apply quantization (Kim et al., 2023; Frantar & Alistarh, 2023). For memory-constrained settings, offloading methods like MoE-Infinity (Xue et al., 2024) cache experts between CPU and GPU. MoE-Spec applies on top of compressed or offloaded models.

Speculative Decoding for MoE. MoE verification cost scales with draft complexity, creating tension between speculation depth and efficiency. Saxena et al. (2025) address this by adapting speculation length dynamically, disabling speculation when overhead exceeds benefit. However, their approach targets chain-structured drafts with lengths $K \leq 3$, where expert activation remains moderate.

Modern tree-structured methods like EAGLE-3 use draft trees of 60+ tokens. At this scale, OLMoE activates 54 of 64 experts per layer on average; even modest trees saturate expert activation, limiting what adaptive length can achieve. MoE-Spec takes a different approach: rather than backing off speculation when verification is expensive, we reduce verification cost directly by budgeting experts.

In memory-constrained settings, SP-MoE (Chen et al., 2025) uses the drafting stage to prefetch experts via cross-model prediction, while SpecMoEOff (Wang et al., 2025) employs

speculative decoding to amortize CPU-GPU transfer costs. These offloading methods target PCIe bottlenecks; MoE-Spec targets HBM bandwidth when experts fit in GPU memory.

6. Limitations

MoE-Spec introduces an expert budget hyperparameter that must be selected per deployment. At well-chosen budgets, quality matches EAGLE-3 while improving speedup (Table 1); very aggressive budgets can degrade quality, and the Pareto curves in Figure 10 show the full tradeoff space to guide budget selection. The router-based ranking requires computing routing probabilities for all experts across the draft tree before verification, adding 2–3% overhead; for very small draft trees, this overhead may outweigh the savings from reduced expert loading. We evaluate single-request inference on A100 GPUs, but batch inference changes the tradeoffs: when multiple requests share experts, the marginal cost of loading additional experts decreases, so expert budgeting may provide smaller gains in high-throughput batch serving scenarios.

Our experiments use top- k softmax routing, which is standard in OLMoE, Qwen3, and Mixtral; some recent architectures such as DeepSeek-V3 use sigmoid-based routing with auxiliary-loss-free load balancing, and the aggregation strategy in Equation (5) may need adaptation for these routing schemes. We do not adapt the budget per layer; some MoE layers may tolerate tighter budgets than others, and per-layer adaptation could improve the quality-speedup tradeoff. Additionally, router-based selection treats experts independently; methods that model expert co-activation could close the gap with Oracle selection (Section 4.5). We leave these directions to future work.

7. Conclusion

Expert routing during MoE verification is heavy-tailed: most of the bandwidth goes to experts that contribute little to output quality. MoE-Spec exploits this by enforcing an expert budget, loading only the highest-scoring experts and dropping the long tail. This decouples verification cost from draft tree complexity, yielding 10–30% throughput gains over EAGLE-3 across three MoE architectures.

The method requires no learned predictor or auxiliary model. The router already provides importance scores; aggregating them across the draft tree identifies which experts to load. Our Oracle analysis suggests that modeling expert co-activation, rather than scoring experts independently, could push budgets lower still. This points to a natural extension: selection methods that exploit the correlation structure we observe in expert routing.

Impact Statement

This paper presents work whose goal is to advance the field of machine learning. There are many potential societal consequences of our work, none of which we feel must be specifically highlighted here.

References

Achiam, J., Adler, S., Agarwal, S., Ahmad, L., Akkaya, I., Aleman, F. L., Almeida, D., Altenschmidt, J., Altman, S., Anadkat, S., et al. Gpt-4 technical report. arXiv preprint arXiv:2303.08774, 2023.

Cai, T., Li, Y., Geng, Z., Peng, H., Lee, J. D., Chen, D., and Dao, T. Medusa: Simple llm inference acceleration framework with multiple decoding heads. arXiv preprint arXiv:2401.10774, 2024.

Chen, C., Borgeaud, S., Irving, G., Lespiau, J.-B., Sifre, L., and Jumper, J. Accelerating large language model decoding with speculative sampling. arXiv preprint arXiv:2302.01318, 2023.

Chen, L., Wen, Z., Wu, T., Zhang, X., and Wu, C. Sp-moe: Speculative decoding and prefetching for accelerating moe-based model inference, 2025. URL <https://arxiv.org/abs/2510.10302>.

Fedus, W., Zoph, B., and Shazeer, N. Switch transformers: Scaling to trillion parameter models with simple and efficient sparsity. *Journal of Machine Learning Research*, 23(120):1–39, 2022.

Frantar, E. and Alistarh, D. Qmoe: Practical sub-1-bit compression of trillion-parameter models. *arXiv preprint arXiv:2310.16795*, 2023.

Gale, T., Narayanan, D., Young, C., and Zaharia, M. Megablocks: Efficient sparse training with mixture-of-experts. *Proceedings of Machine Learning and Systems*, 5:288–304, 2023.

Guo, D., Yang, D., Zhang, H., Song, J., Wang, P., Zhu, Q., Xu, R., Zhang, R., Ma, S., Bi, X., et al. Deepseek-r1: Incentivizing reasoning capability in llms via reinforcement learning. *arXiv preprint arXiv:2501.12948*, 2025.

Jiang, A. Q., Sablayrolles, A., Roux, A., Mensch, A., Savary, B., Bamford, C., Chaplot, D. S., Casas, D. d. l., Hanna, E. B., Bressand, F., et al. Mixtral of experts. arXiv preprint arXiv:2401.04088, 2024.

Kim, Y. J., Fahim, R., and Awadalla, H. H. Mixture of quantized experts (moqe): Complementary effect of low-bit quantization and robustness. *arXiv preprint arXiv:2310.02410*, 2023.

Leviathan, Y., Kalman, M., and Matias, Y. Fast inference from transformers via speculative decoding. In *Proceedings of the 40th International Conference on Machine Learning*, volume 202 of *Proceedings of Machine Learning Research*, pp. 19274–19286. PMLR, 23–29 Jul 2023.

Li, P., Zhang, Z., Yadav, P., Sung, Y.-L., Cheng, Y., Bansal, M., and Chen, T. Merge, then compress: Demystify efficient SMoe with hints from its routing policy. In *International Conference on Learning Representations*, 2024a. URL <https://openreview.net/forum?id=eFWG9Cy3WK>.

Li, Y., Wei, F., Zhang, C., and Zhang, H. Eagle: Speculative sampling requires rethinking feature uncertainty. arXiv preprint arXiv:2401.15077, 2024b.

Li, Y., Wei, F., Zhang, C., and Zhang, H. Eagle-2: Faster inference of language models with dynamic draft trees. In *Proceedings of the 2024 conference on empirical methods in natural language processing*, pp. 7421–7432, 2024c.

Li, Y., Wei, F., Zhang, C., and Zhang, H. Eagle-3: Scaling up inference acceleration of large language models via training-time test. In *The Thirty-ninth Annual Conference on Neural Information Processing Systems*, 2025.

Liu, Z., Wang, J., Dao, T., Zhou, T., Yuan, B., Song, Z., Shrivastava, A., Zhang, C., Tian, Y., Re, C., et al. Deja vu: Contextual sparsity for efficient llms at inference time. In *International Conference on Machine Learning*, pp. 22137–22176. PMLR, 2023.

Meta AI. The llama 4 herd: The beginning of a new era of natively multimodal ai innovation, 2025. URL <https://ai.meta.com/blog/llama-4-multimodal-intelligence/>.

Muennighoff, N., Soldaini, L., Groeneveld, D., Lo, K., Morrison, J., Min, S., Shi, W., Walsh, E. P., Tafjord, O., Lambert, N., et al. Olmoe: Open mixture-of-experts language models. In *The Thirteenth International Conference on Learning Representations*, 2024.

Saxena, A., Tsai, P.-A., Taneja, H., Jaleel, A., and Qureshi, M. Utility-driven speculative decoding for mixture-of-experts, 2025. URL <https://arxiv.org/abs/2506.20675>.

Shazeer, N., Mirhoseini, A., Maziarz, K., Davis, A., Le, Q., Hinton, G., and Dean, J. Outrageously large neural networks: The sparsely-gated mixture-of-experts layer. arXiv preprint arXiv:1701.06538, 2017.

Song, Y., Mi, Z., Xie, H., and Chen, H. Powerinfer: Fast large language model serving with a consumer-grade gpu. In *Proceedings of the ACM SIGOPS 30th Symposium on Operating Systems Principles*, pp. 590–606, 2024.

Wang, Z., Zhang, Z., Zhou, Y., Wang, Z., Zhou, M., Jiang, P., Cai, W., Huan, C., Gu, R., Zhong, S., and Tian, C. Accelerating mixture-of-experts inference by hiding offloading latency with speculative decoding, 2025. URL <https://arxiv.org/abs/2508.21706>.

Xie, Y., Zhang, Z., Zhou, D., Xie, C., Song, Z., Liu, X., Wang, Y., Lin, X., and Xu, A. Moe-pruner: Pruning mixture-of-experts large language model using the hints from its router. *arXiv preprint arXiv:2410.12013*, 2024.

Xue, L., Fu, Y., Lu, Z., Mai, L., and Marina, M. Moe-infinity: Offloading-efficient moe model serving. *arXiv preprint arXiv:2401.14361*, 2024.

A. Hyperparameters

Table 2 summarizes the general experimental settings. Table 3 provides model-specific configurations. Note that we use conservative budget ranges for $T = 1$ experiments (as reported in Section 4.1) and explore the fuller ranges shown in the table for $T = 0$ experiments.

Draft Tree Size. We use a default draft tree size of 63 tokens, following the EAGLE-3 configuration. The tree size sweep (3–511) in Figure 4 shows that MoE-Spec’s speedup grows with tree size, since larger trees activate more unique experts under standard verification. The choice of 63 balances acceptance rate against verification overhead for the baseline.

Expert Budget Selection. Budget ranges are model-specific based on the expert configuration. For OLMoE (64 experts, $k=8$), we sweep $B \in \{8, 16, 24, 32, 40, 48, 56\}$; the minimum of 8 ensures at least one full set of active experts. For Qwen3 (128 experts, $k=8$), we use $B \in \{16, 24, 32, 48, 64\}$. Mixtral’s smaller expert pool (8 experts, $k=2$) limits the range to $B \in \{2, 3, 4, 5, 6, 7\}$. Main results (Table 1) report the budget maximizing speedup while maintaining quality within one standard deviation of EAGLE.

Reproducibility. For $T=1$ experiments, we report mean and standard deviation over 5 random seeds. All models use FP16 precision. We use PyTorch 2.1 with CUDA 12.1. Model weights are loaded from HuggingFace Hub; draft model adapters are from the official EAGLE repository.

B. MoE-Spec Algorithm

Algorithm 1 provides pseudocode for verification-time expert budgeting. The algorithm has three stages: (1) compute routing probabilities for all tokens in the draft tree, (2) aggregate importance scores per expert by summing routing

Table 2. General experimental settings.

Parameter	Value
Draft tree size (main)	63
Draft tree size (sweep)	3–511
Decoding temperature	0.0, 1.0
Samples per benchmark	80
Max generation length	1024
Shortlist method	Router
Token policy	Substitution
GPU type	NVIDIA A100
GPU memory	80GB

Table 3. Model-specific configurations.

Model	Experts	Budget (B)	Draft / GPUs
OLMoE-1B-7B	64 ($k=8$)	8–56	EAGLE-3 / 1
Qwen3-30B-A3B	128 ($k=8$)	16–64	EAGLE-3 / 1
Mixtral-8x7B	8 ($k=2$)	2–7	EAGLE / 2

probabilities, and (3) apply the token policy (truncation or substitution) using only the top- B experts. The aggregation step requires no additional model execution beyond what the router already computes.

Algorithm 1 MoE-Spec Expert Budgeting

Input: Hidden states $\{\mathbf{h}_1, \dots, \mathbf{h}_M\}$, budget B , policy
Output: MoE output for each token

```

// Compute routing probabilities
for  $t = 1, \dots, M$  do
     $g_i(\mathbf{h}_t) \leftarrow \text{softmax}(\mathbf{W}_{\text{gate}} \mathbf{h}_t)$  for all  $i$ 
// Aggregate importance scores
for  $i = 1, \dots, N$  do
     $s_i \leftarrow \sum_{t=1}^M g_i(\mathbf{h}_t)$ 
// Select shortlist
 $\mathcal{S} \leftarrow \text{top-}B$  experts by  $s_i$ 
// Apply token policy
for  $t = 1, \dots, M$  do
    if policy = truncation then
         $\mathcal{T}_k(\mathbf{h}_t) \leftarrow \text{top-}k$  experts by  $g_i(\mathbf{h}_t)$ 
         $\text{out}_t \leftarrow \sum_{i \in \mathcal{T}_k(\mathbf{h}_t) \cap \mathcal{S}} \bar{g}_i(\mathbf{h}_t) \cdot E_i(\mathbf{h}_t)$ 
    else // substitution
         $\mathcal{T}_k^S(\mathbf{h}_t) \leftarrow \text{top-}k$  in  $\mathcal{S}$  by  $g_i(\mathbf{h}_t)$ 
         $\text{out}_t \leftarrow \sum_{i \in \mathcal{T}_k^S(\mathbf{h}_t)} \bar{g}_i^S(\mathbf{h}_t) \cdot E_i(\mathbf{h}_t)$ 
return  $\{\text{out}_1, \dots, \text{out}_M\}$ 

```

C. Batched MoE Computation

We use the open-source EAGLE-3 implementation without modification to tree construction or verification logic. Our only change is to the MoE computation: the reference EA-

Table 4. Comparison of sequential vs. batched MoE computation on OLMoE-1B-7B (EAGLE-3, no expert budget). Quality differences are within noise; throughput improves 1.4–1.5×.

Benchmark	Mode	Quality	Throughput	Accept
GSM8K	Sequential	0.663	17.1 tok/s	2.98
	Batched	0.688	25.2 tok/s	3.00
HumanEval	Sequential	0.304	23.6 tok/s	4.16
	Batched	0.304	35.0 tok/s	4.20
CNN/DM	Sequential	0.180	12.3 tok/s	1.93
	Batched	0.173	18.4 tok/s	1.96

GLE implementation processes experts sequentially, gathering tokens routed to each expert, computing the expert output, and accumulating results via `index_add_`. This approach is simple but inefficient, as it issues many small matrix multiplications.

We implement batched expert computation, which processes all active experts in parallel using batched matrix multiplications. Given the set of active experts \mathcal{E} , we stack their weight matrices and compute all expert outputs in a single batched `matmul` operation. This reduces kernel launch overhead and better utilizes GPU parallelism.

Table 4 compares the two execution modes on OLMoE-1B-7B across three benchmarks. The batched implementation provides 1.4–1.5× higher throughput with negligible difference in task quality (within run-to-run variance), confirming our optimization does not affect model accuracy. We apply batched execution uniformly to all methods, including AR and EAGLE-3 baselines, to ensure fair comparison.

D. Expert Co-activation Analysis

To understand why Oracle selection outperforms Router-based selection (Section 4.5), we analyze expert co-activation patterns during inference. Co-activation measures how often pairs of experts are selected together for the same token. If certain expert pairs frequently co-activate, their outputs are correlated, and selecting both provides diminishing marginal returns.

Methodology. We run inference on 50 samples from each benchmark (GSM8K, HumanEval, MATH500, MBPP, CNN/DM) using OLMoE-1B-7B with EAGLE-3 speculative decoding. For each token processed during verification, we record which experts appear in its top- k selection. For each MoE layer, we build a 64×64 co-activation matrix where entry (i, j) counts how many times experts i and j were both selected for the same token.

Concentration Metric. We measure routing concentration as the ratio between the most frequent co-activating pair and the expected count under uniform-random selection.

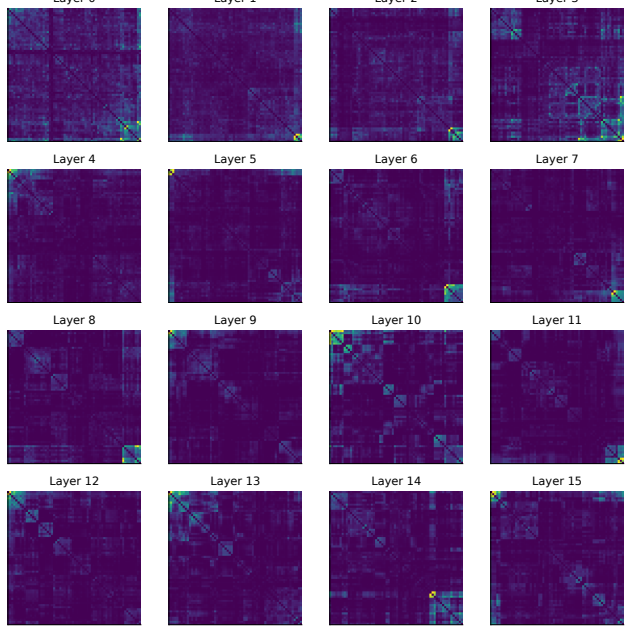


Figure 8. Expert co-activation heatmaps for all 16 MoE layers in OLMoE-1B-7B. Each cell shows normalized pairwise co-activation frequency. Experts are reordered by hierarchical clustering. Bright diagonal blocks indicate expert groups that frequently activate together, with concentration ratios of 10–33× above uniform-random expectation.

Under uniform selection of $k = 8$ experts from $N = 64$, the probability that any specific pair (i, j) both appear is $\frac{k(k-1)}{N(N-1)} \approx 0.014$. If all pairs were equally likely, each would have the same expected count. The concentration ratio is:

$$\text{Concentration} = \frac{\max_{i,j} \text{coact}(i, j)}{\text{expected per pair}} \quad (9)$$

Results. Figure 8 shows co-activation heatmaps for all 16 MoE layers. Experts are reordered using hierarchical clustering to reveal structure. Across layers, certain expert groups co-activate far more frequently than random: concentration ratios range from 10× to 33× (mean 23×). The bright diagonal blocks indicate expert clusters that frequently appear together.

This concentration explains the Oracle-Router gap. Router-based selection scores experts independently, so it tends to select multiple experts from the same high-frequency cluster. Oracle selection, which greedily minimizes reconstruction error, avoids this redundancy: after selecting one expert from a cluster, remaining cluster members provide less marginal error reduction and are passed over in favor of experts covering different parts of the output space.

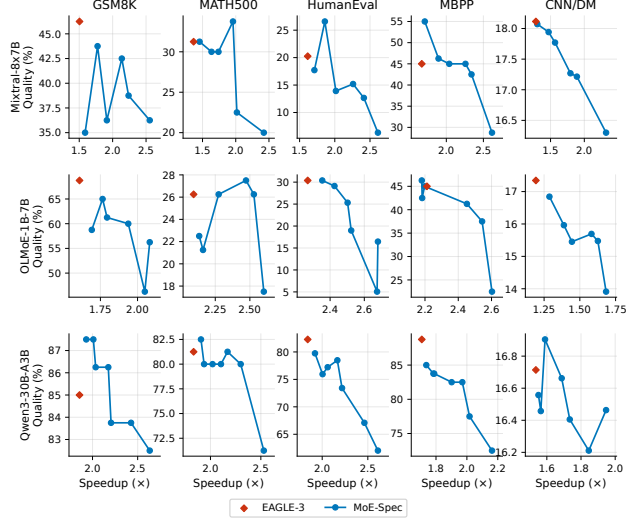


Figure 9. Quality vs. speedup at $T = 0$ across three models (rows) and five benchmarks (columns). Diamonds mark EAGLE; connected points show MoE-Spec at varying expert budgets.

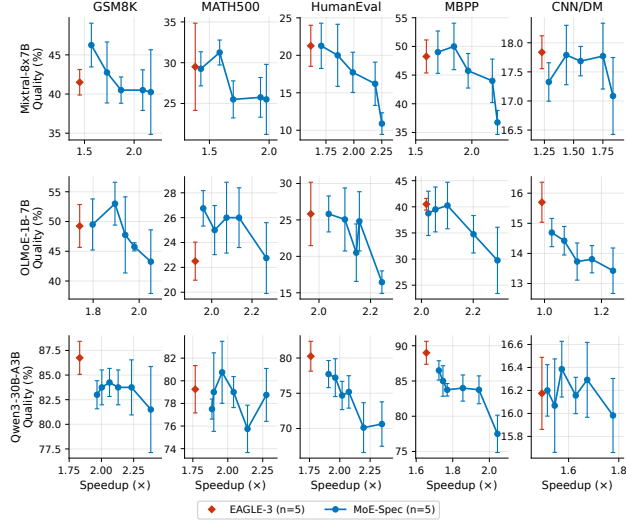


Figure 10. Quality vs. speedup at $T = 1$ across three models (rows) and five benchmarks (columns). Error bars show standard deviation over 5 seeds.

E. Quality-Speedup Tradeoffs by Benchmark

Figures 9 and 10 show the full quality-speedup tradeoff across all model-benchmark combinations at temperatures $T = 0$ and $T = 1$. Each panel plots task quality against speedup relative to autoregressive decoding. Diamonds mark EAGLE-3 (or EAGLE-1 for Mixtral); connected points trace MoE-Spec across expert budgets.

At $T = 0$ (greedy decoding), there is no sampling variance, so each point represents a single deterministic evaluation. At $T = 1$, error bars show standard deviation over 5 seeds. In both settings, MoE-Spec extends the Pareto frontier to

higher speedups, with quality degradation only at aggressive budgets.

Generally, we find that code generation (HumanEval, MBPP) tolerates tighter budgets than reasoning (GSM8K, MATH500). This matches the coverage analysis in Section 4.6: code tasks concentrate routing on fewer experts, so budgeting removes less relevant capacity. Summarization (CNN/DM) falls between: routing is dispersed but the task is less sensitive to small output perturbations.